

Under these assumptions, the invertibility principle can be expressed in the following way. If (22) is differentiated with respect to r , using (24), (25) and the assumption of constant f , the result after multiplication by σ can be written as

$$\frac{\partial}{\partial r} \left[\frac{1}{r} \frac{\partial(rv)}{\partial r} \right] - \frac{\zeta_{a\theta}}{\sigma} \frac{\partial \sigma}{\partial r} = \sigma \frac{\partial P}{\partial r}. \quad (26)$$

Differentiating (23) with respect to r and making use of the thermal wind equation (21), we get

$$-g \frac{\partial \sigma}{\partial r} = \frac{\partial^2 p}{\partial r \partial \theta} = \frac{\partial}{\partial \theta} \left[\frac{f_{\text{loc}}}{R} \frac{\partial v}{\partial \theta} \right]. \quad (27)$$

(For later reference, the relation between R , σ and the static stability can be shown to be

$$R = g/(\sigma N^2 \theta^2) > 0, \quad (28)$$

N^2 being the static stability expressed as the square of the Brunt-Väisälä or buoyancy frequency.) Using (22) and (27), we can write (26) finally as

$$\frac{\partial}{\partial r} \left[\frac{1}{r} \frac{\partial(rv)}{\partial r} \right] + g^{-1} P \frac{\partial}{\partial \theta} \left(\frac{f_{\text{loc}}}{R} \frac{\partial v}{\partial \theta} \right) = \sigma \frac{\partial P}{\partial r} \quad (29)$$

a nonlinear equation which can be solved, for instance by relaxation methods, as described below, for the wind profile $v(r, \theta)$ given the PV distribution $P(r, \theta)$. Note that the *isentropic gradient* of P appears on the right-hand side as a prescribed forcing function.

Together with suitable boundary conditions, and the condition (17a), Eq. (29) expresses the invertibility principle in much the same way as was done in Kleinschmidt's original work. Note that if

$$f_{\text{loc}} P > 0, \quad (30)$$

as we shall assume, then Eq. (29) is an elliptic equation, so that the problem is well posed. As is well known, (30), together with (23), also expresses the assumption of static, inertial, and 'symmetric' baroclinic stability previously made in section 1(d) (e.g. Hoskins 1974, with f replaced by f_{loc}). Equation (29) is exact; its simple form is due to the assumption of circular symmetry and the use of isentropic coordinates.

Note further that if we were to make the approximations

$$f_{\text{loc}} \approx \zeta_{a\theta} = f, \quad R \approx R_{\text{ref}}(\theta), \quad \sigma \approx \sigma_{\text{ref}}(\theta) \quad (31)$$

everywhere except when calculating the forcing function $\partial P/\partial r$ from (22), where $R_{\text{ref}}(\theta)$ and $\sigma_{\text{ref}}(\theta)$ are the reference-state profiles of R and σ , then (29) would simplify to

$$\frac{\partial}{\partial r} \left(\frac{1}{r} \frac{\partial(rv)}{\partial r} \right) + \frac{f^2}{g \sigma_{\text{ref}}} \frac{\partial}{\partial \theta} \left(R_{\text{ref}}^{-1} \frac{\partial v}{\partial \theta} \right) = \sigma_{\text{ref}} \frac{\partial P}{\partial r}, \quad (32)$$

which is the isentropic coordinate version of the usual quasi-geostrophic approximation to (29). The elliptic operator on the left-hand side of (32) is now linear and if, further, σ_{ref} and R_{ref} were constants, then apart from its slightly different r -dependence the operator would be a three-dimensional Laplacian, after suitably rescaling the vertical coordinate according to the Prandtl-Rossby-Burger relation

$$\Delta \theta \sim fL/(Rg\sigma)^{1/2} \quad (\text{cf. } H \sim fL/N) \quad (33a)$$

(e.g. Rossby 1938), where L is the horizontal scale of the flow. For a more accurate scale relation corresponding to (29) we may replace f by $(f_{\text{loc}}P\sigma)^{1/2}$, giving

$$\Delta\theta \sim (f_{\text{loc}}P/Rg)^{1/2}L \quad (\text{cf. } H \sim (f_{\text{loc}}P\sigma)^{1/2}L/N), \quad (33b)$$

which would be relevant near the equator. H and $\Delta\theta$ are respectively the scales in physical, xyz space and in $xy\theta$ space, measuring the vertical penetration of the induced flow structure above or below the location of the IPV anomaly. The relevance of $\Delta\theta$ rather than H in the isentropic coordinate description explains why the square of the Brunt-Väisälä frequency appears in the denominator, rather than the numerator of (28).

We shall call the expressions on the right of (33a) the Rossby heights (in $xy\theta$ and xyz space respectively), and denote them by $\Delta\theta_{\text{Rossby}}$ and H_{Rossby} . As is well known, the concept is complementary to that of the Rossby radius of deformation, which is the horizontal scale L obtained from (33a) when $\Delta\theta$ or H is given. If $\Delta\theta_{\text{Rossby}}$ and H_{Rossby} greatly exceed the corresponding reference-density scale heights $\Delta\theta_{\text{density}}$, H_{density} (the scale heights for variation of σ and ρ respectively), then non-Boussinesq effects are important. Order-of-magnitude relations which cover the whole range of $\Delta\theta$ or H are

$$\Delta\theta \sim \min\{\Delta\theta_{\text{Rossby}}, \Delta\theta_{\text{density}}\} \quad \text{and} \quad H \sim \min\{H_{\text{Rossby}}, H_{\text{density}}\} \quad (33c)$$

for the vertical scales for downward penetration of the induced wind field, and

$$\Delta\theta \sim \max\left\{\Delta\theta_{\text{Rossby}}, \frac{(\Delta\theta_{\text{Rossby}})^2}{\Delta\theta_{\text{density}}}\right\} \quad \text{and} \quad H \sim \max\left\{H_{\text{Rossby}}, \frac{(H_{\text{Rossby}})^2}{H_{\text{density}}}\right\} \quad (33d)$$

for its upward penetration (Rossby, *op. cit.*). These more general scaling rules are related to well-known results in tidal theory.*

The fact that the inverse Laplacian is a smoothing operator should be kept in mind; for instance it is the essential reason why Figs. 4, 6 and 12 look like smoothed versions of Figs. 3, 5 and 11 (see also (44) below). There is an associated *scale effect*, whereby small-scale features of given strength in the IPV field have a relatively weak effect on the velocity field whereas large-scale features have a relatively strong effect. As already mentioned, this is one of the reasons for supposing that coarse-grain IPV distributions are dynamically meaningful. Note that the smoothing takes place in the vertical as well as in the horizontal.

The exact operator appearing in (29) is nonlinear because of the presence of the unknown functions f_{loc} , R and σ (σ appearing on the right-hand side). As Figs. 3, 4, 5, 6, 11 and 12 suggest, this operator very often has the same qualitative character as its approximate counterpart in (32), although it should be remembered that differences near fronts and shear lines can be important (e.g. Hoskins and Bretherton 1972). In many circumstances of interest, (29) may be expected to be soluble iteratively, for given $P(r, \theta)$, having regard to any constraint imposed via (17b). The conceptually simplest albeit not

* The alternatives within braces are the asymptotic forms for large and small $H_{\text{density}}/H_{\text{Rossby}}$, as the case may be, of the more precise expression

$$H = |(2H_{\text{density}})^{-1} \pm \sqrt{(H_{\text{Rossby}})^{-2} + (2H_{\text{density}})^{-2}}|^{-1},$$

the + and - signs corresponding to downward and upward penetration respectively, which arises in the theory of very-low-frequency tidal oscillations of negative equivalent depth (Kato 1966; Lindzen 1966). The problem solved by Rossby (1938) is an approximate version of the same problem; both concern the linear response to a forcing effect of a given horizontal scale L at a given level. A convenient reference is Holton (1975), in which it should be noted that the expression (2.85) corresponds apart from sign convention to minus the square of the expression

$$\sqrt{(H_{\text{Rossby}})^{-2} + (2H_{\text{density}})^{-2}}$$

above, H_{Rossby} being equal to $\sqrt{-gh/N^2}$ in Holton's notation, where h is the equivalent depth.

the most powerful method starts from a solution to (32) as first guess, and then refines the initial approximations (31) by straightforward iteration. Notice carefully how the condition (17a) invoking the reference state has to enter into this process. As soon as a guess for $v(r, \theta)$ has been computed from (29), using the previous guesses for $R(p) = R(r, \theta)$, and $\sigma(r, \theta)$, improved approximations to $R(r, \theta)$ and $\sigma(r, \theta)$ must be derived

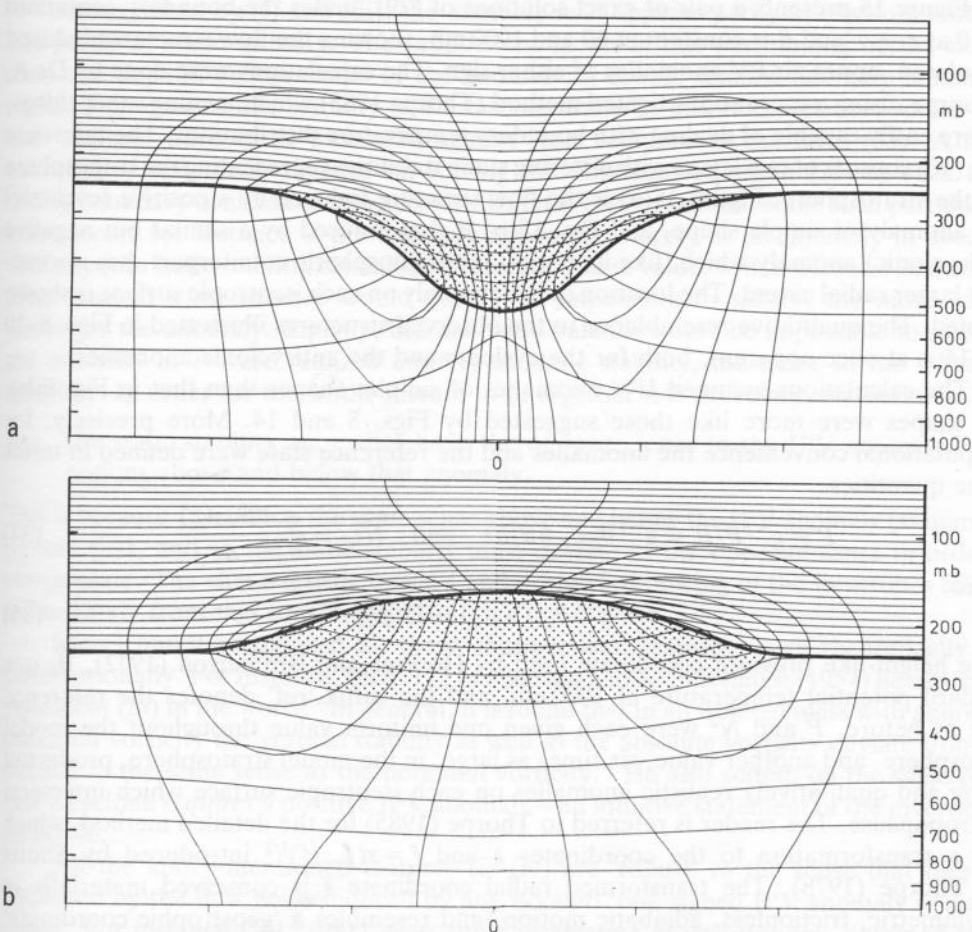


Figure 15. Circularly symmetric flows induced by simple, isolated, IPV anomalies (whose locations are shown stippled) as described in the text. The basic static stability \bar{N} and therefore \bar{P} (defined in (34)) was uniform in the tropospheric region and six times larger in the stratospheric region. The vertical coordinate z is nearly the same as physical height but is defined exactly in (35), g/θ_0 being taken to be $(1/30) \text{ m s}^{-2} \text{ K}^{-1}$. The reference tropospheric 'height' z was 10 km and the total domain 'height' 16.67 km: f was taken to be 10^{-4} s^{-1} . The IPV anomaly was defined by taking the tropopause potential temperature to vary in the manner $\frac{1}{2}A\{\cos(\pi\tilde{r}/r_0) + 1\}$ for $\tilde{r} < r_0$, where $\tilde{r} = r(f_{loc}/f)^{1/2}$. Here the amplitude A was taken to be -24 K in (a) and $+24 \text{ K}$ in (b) which may be compared with a potential temperature increase of 30 K over the depth of the reference troposphere. The parameter r_0 was taken to be 1667 km. The undisturbed θ distribution was imposed as a boundary condition at $\tilde{r} = 5000 \text{ km}$, and the solutions obtained had only a weak dependence of $C_b(\theta)$ upon θ as well as a far-field stratification approximating the reference stratification (16). (In terms of our definitions, the IPV anomaly in the stippled regions must therefore strictly speaking be considered to be embedded in a suitable 'surround' of much weaker anomalies, as noted below (17b).) Only the region $r < 2500 \text{ km}$ is shown here, and the tick marks below the axes are drawn every 833 km. The thick line represents the tropopause and the two sets of thin lines the isentropes every 5 K and the transverse velocity every 3 m s^{-1} . The zero isotach on the axis of symmetry is omitted. In (a) the sense of the azimuthal wind is cyclonic and in (b) it is anticyclonic, in both cases the maximum contour value being 21 m s^{-1} . The surface pressure anomaly is -41 mb in (a) and $+13 \text{ mb}$ in (b) and the relative vorticity extrema (located at the tropopause) are $1.7f$ in (a) and $-0.6f$ in (b). The maximum surface winds are 15 m s^{-1} and 6 m s^{-1} respectively. For more details of the method of computation, see Thorpe (1985).

Courtesy of A. J. Thorpe.

for use in the next iteration. This requires (18a) to be integrated with respect to r , after which (18b) and (19a) are used to get $p(r, \theta)$ followed by (20) and (23) to get R and θ . When (18a) is integrated with respect to r , an arbitrary function of θ arises as a function of integration, and the reference-state condition (17a), along with the boundary conditions, is needed to determine this function of integration.

Figure 15 presents a pair of exact solutions of (29), under the boundary conditions $v \rightarrow 0$ as $r \rightarrow \infty$ and $\theta = \text{constant}$ at 60 and 1000 mb, showing the flow structures induced by isolated, upper air PV anomalies of either sign. The calculations were done by Dr J. Thorpe, using a more sophisticated method (Thorpe 1985) which, among other things, is more easily capable of dealing with boundary temperature distributions. The reference state (16) consists of two layers with differing static stabilities representing the troposphere and the stratosphere. Figure 15(a) is the flow structure induced by a positive (cyclonic) IPV anomaly of simple shape, and Fig. 15(b) is that induced by a similar but negative (anticyclonic) anomaly which, like its typical real-atmospheric counterpart, has a somewhat larger radial extent. The location of the anomaly on each isentropic surface is shown stippled. The qualitative resemblance to the observed structures illustrated in Figs. 8 and 14 is at once apparent, both for the cyclonic and the anticyclonic anomalies.

The calculations assumed IPV anomalies of simpler shapes than that in Fig. 9(b). The shapes were more like those suggested by Figs. 8 and 14. More precisely, for computational convenience the anomalies and the reference state were defined in terms of the quantities

$$\tilde{P} = g^{-1}P/R = g^{-1}\theta_0\zeta_{a\theta}\partial\theta/\partial z \quad \text{and} \quad \tilde{N}_{\text{ref}}^2 = \frac{g}{\theta_0} \frac{d\theta_{\text{ref}}(z)}{dz} \quad (3)$$

where

$$z = g^{-1}\theta_0\{\Pi(p_0) - \Pi(p)\} \quad (3)$$

is the height-like pressure coordinate used by Hoskins and Bretherton (1972), θ_0 is the standard potential temperature at 1000 mb, and the suffix 'ref' denotes the reference state as before. \tilde{P} and \tilde{N}^2 were each given one uniform value throughout the model troposphere, and another value, six times as large, in the model stratosphere, producing strong and qualitatively realistic anomalies on each isentropic surface which intersect the tropopause. The reader is referred to Thorpe (1985) for the detailed method, which uses a transformation to the coordinates z and $\tilde{r} = r(f_{\text{loc}}/f)^{1/2}$ introduced by Shutt and Thorpe (1978). The transformed radial coordinate \tilde{r} is conserved materially in axisymmetric, frictionless, adiabatic motion, and resembles a 'geostrophic coordinate' (Hoskins 1975, Blumen 1981) except that gradient-wind rather than geostrophic balance is used. Some quantitative details of the calculations are given in the caption to Fig. 15. Note for instance that the values of f_{loc} and the absolute isentropic vorticity $\zeta_{a\theta}$ greatly exceed f near the centre of the cyclonic vortex; for this and other reasons both quasi-geostrophic and semi-geostrophic theory (sections 5(b), (c) below) would be poor approximations.

Qualitative features to be especially noted about Figs. 15(a), (b) include the facts that:

- (i) the circulation in the balanced vortex has the same sense, relative to the earth, as the IPV anomaly which induces it;
- (ii) the induced fields penetrate vertically above and below the IPV anomaly, boundary constraints permitting, by amounts consistent with the scale relations (33), especially when f is replaced by $(f_{\text{loc}}P\sigma)^{1/2}$ as in (33b), and
- (iii) the static stability N^2 , as well as the absolute vorticity, is anomalously high within a high PV anomaly, and low within a low PV anomaly, relative to the static stability of the reference state.

Note that for this purpose the 'anomaly' in the static stability, being the anomaly relative to the reference state, means *isentropic* anomaly, just as it does for P itself; one is comparing the static stability in the centre of the IPV anomaly with the static stability on the same isentropic surface at the periphery of the picture, where the actual state approximates the reference state.

As suggested by (i) and (iii), the anomaly in P appears partly as absolute vorticity and partly as static stability. The proportions in which this partitioning occurs can be shown to depend on the shape of the anomaly, a broad, shallow anomaly tending to realize P more as static stability and a tall one more as absolute vorticity, where 'tall' and 'shallow' have to be measured against scale relations of the form (33). A more quantitative statement depends on solving the nonlinear equation (29) in each case, taking boundary constraints into account. But it is easy to see that some such partitioning must occur; for instance if the anomaly appeared entirely as an anomaly in absolute vorticity (the static stability retaining its reference-state value, with horizontal isentropes) then thermal wind balance would plainly be impossible to satisfy, the more so the shallower the anomaly. Equally, thermal wind balance would be impossible to satisfy if the anomaly in P were realized entirely as static stability, the more so the taller the anomaly. In order for the whole picture to fit together it is necessary, furthermore, that

- (iv) the static stability anomalies have the *opposite* sense to the IPV anomaly in the regions above and below that anomaly.

This is because $\zeta_{a\theta}$ still has the same sense above and below the IPV anomaly (statements (i) and (ii)), and so the static stability must deviate in the opposite sense in order to compensate. The characteristic upward and downward bowing of the isentropes follows immediately from this consideration.

Kleinschmidt recognized all these characteristic features, both theoretically and observationally. For instance, on p. 115 of Eliassen and Kleinschmidt (1957) he expressed statement (iii) in the words "In general, it is found that in an isolated mass with abnormal potential vorticity the vertical stability as well as the absolute vorticity deviate from the normal in the same sense as the potential vorticity." He also stated, on the same page, that a cyclone *requires* a positive IPV anomaly—an intuitive statement of the invertibility principle.

All the above-mentioned features (i)–(iv) are 'robust' in the sense that they are exhibited by the flow fields induced by any isolated, one-signed IPV anomaly of simple shape. For instance Gill (1981) gives some interesting exact solutions, obtained by an elegant analytical method, for very strong, anticyclonic, two-dimensional IPV anomalies. In each case the PV in the anomaly is *zero*, and the anomaly is concentrated on a single isentropic surface. All the qualitative features (i)–(iv) are reproduced even in that extreme limiting case. They are likewise reproduced by solutions to the approximate equation (32), which are valid for a sufficiently *weak* anomaly. For instance, let R_{ref} and σ_{ref} be taken to be constants in (32) (a Boussinesq, quasi-geostrophic model with a constant-static-stability reference state) and let P be taken to be constant and to be equal to $\sigma_{\text{ref}}^{-1}f(1 + \epsilon)$, with $\epsilon \ll 1$, within an ellipsoidal region $r^2 + \Theta^2 = C^2 = \text{constant}$, and to have its reference value $\sigma_{\text{ref}}^{-1}f$ outside that region, where Θ is the scaled coordinate $f^{-1}(R_{\text{ref}}g\sigma_{\text{ref}})^{1/2}(\theta - \theta_c)$, cf. (33a), θ_c being the value of θ at the centre of the ellipsoidal region. Then it is a straightforward theoretical exercise to construct an analytical solution, again exhibiting the same features (i)–(iv), in which

$$\left. \begin{aligned} v &= \frac{1}{3}\epsilon fr & (r^2 + \Theta^2 < C^2) \\ v &= \frac{1}{3}\epsilon fr \left(\frac{C^2}{r^2 + \Theta^2} \right)^{3/2} & (r^2 + \Theta^2 > C^2) \end{aligned} \right\} \quad (36)$$

